Reduction of Earth Alkaline Metal Salts in THF Solution Studied by Picosecond Pulse Radiolysis

ARTICLE *in* THE JOURNAL OF PHYSICAL CHEMISTRY A · DECEMBER 2013

Impact Factor: 2.69 · DOI: 10.1021/jp410598y · Source: PubMed

6 AUTHORS, INCLUDING:

Jun Ma
Université Paris-Sud 11
15 PUBLICATIONS **79** CITATIONS
SEE PROFILE

Uli Schmidhammer
Université Paris-Sud 11
54 PUBLICATIONS **514** CITATIONS
SEE PROFILE

Pascal Pernot
French National Centre for Scientific Research
140 PUBLICATIONS **1,213** CITATIONS
SEE PROFILE

Mehran Mostafavi
Université Paris-Sud 11
162 PUBLICATIONS **2,901** CITATIONS
SEE PROFILE

THE JOURNAL OF PHYSICAL CHEMISTRY A

Article

pubs.acs.org/JPCA

Reduction of Earth Alkaline Metal Salts in THF Solution Studied by Picosecond Pulse Radiolysis

Jun Ma, Pierre Archirel, Uli Schmidhammer, Jean-Marie Teuler, Pascal Pernot, and Mehran Mostafavi*

Laboratoire de Chimie Physique/ELYSE, CNRS/Université Paris-Sud, Faculté des Sciences d'Orsay, Bât. 349, 91405 Orsay Cedex, France

Supporting Information

ABSTRACT: Picosecond pulse radiolysis of tetrahydrofuran (THF) solutions containing earth alkaline metal salt, $M^{II}(ClO_4)_2$, at different concentrations are performed using two different supercontinua as probe pulse, one covering the visible and another the near-infrared (NIR) down to the visible. Two types of line scan detectors are used to record the absorption spectra in the range from 400 to 1500 nm. Because of the strong overlap between the spectra of the absorbing species in the present wavelength range, global matrices were built for each M^{II} system, by delay-wise binding the matrix for pure THF with the available matrices for this cation. The number of absorbers was assessed by Singular Value Decomposition of the global matrix, and a MCR-ALS analysis with the corresponding number of species was performed. The analysis of the results show clearly that solvated electron reacts with the earth alkaline metal molecule and the product has an optical absorption band very different than that of solvated electron in pure THF. So, contrarily to the case of solution containing free Na^+, in the presence of Mg^{II}, Ca^{II} and Sr^{II} the observed absorption band is not only blueshifted, but its shape is also drastically changed. In fact with Na^+ solvated electron forms a tight-contact pair but with earth alkaline metal cation solvated electron is scavenged by the undissociated molecule $M^{II}(ClO_4)_2$. In order to determine the structure of the absorbing species observed after the electron pulse, Monte Carlo/DFT simulations were performed in the case of Mg^{II}, based on a classical Monte Carlo code and DFT/PCM calculation of the solute. The UV−visible spectrum of the solute is calculated with the help of the TDDFT method. The calculated spectrum is close to the experimental one. It is due to two species, a contact pair and an anion.

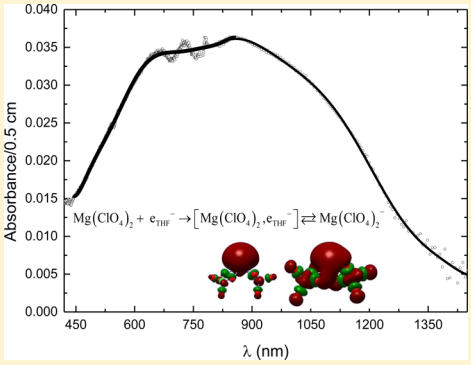

INTRODUCTION

Since 1962, it has been known that the solvated electron can be formed in a variety of solvents.[1−8] The studies of absorption spectra of solvated electron, together with theoretical calculations, showed the existence of several excited states for the hydrated electron.[9−14] The reactivity of solvated electron is very important and the reduction of metal cations in aqueous solution has been extensively studied by pulse radiolysis studies.[15,16] But in comparison, less work has been performed in nonaqueous solutions concerning the reactivity of the solvated electron toward metal cations. In solutions containing nonreactive metal cations, a blue shift of the absorption band of hydrated electron is observed that is due to the formation of a pair between metal cation and hydrated electron. In water, the extent of the blue shift depends on the charge of the nonreactive metal cation and its concentration. For a given concentration of the ion in aqueous solutions, the shift of the absorption band is for example more important for Tb^{3+} than for Mg^{2+} than for Na^+. In ethers, such a spectral shift is also observed when alkaline cations are present in solution. In all cases, in the presence of noncomplexed solvated cations, M^{n+}, the shape of the optical absorption band of the solvated electron is preserved and only the position of the maximum is shifted to the blue side of the absorption spectrum.

Magnesium is an interesting system due to the importance of its reactivity in organic chemistry; among the nonaqueous solvents, tetrahydrofuran (THF) is very often used in organic chemistry, for example, for the formation of the Grignard compounds, RMgX (R, alkyl radical and X, halogen atom), which has been synthesized since the first century.[17] The magnesium metal powder is generally supposed to dissolve and finally form divalent ions in solution during the reaction with RX compounds.[18,19] Still, the involvement of the monovalent magnesium(I), Mg^I, species is discussed as transient in the Grignard compounds formation.[20] Moreover, the magnesium is also supposed to play an important role in electron transfer by enzymatic catalysis. Therefore, it is interesting to understand well the reactivity of this metal cation.

By nanosecond pulse radiolysis study, we reported a possible reaction between solvated electron and Mg^{II}, Ca^{II}, and Sr^{II} in ethers.[21,22] It is important to note that in THF the metal cations remains complexed by counterions ClO_4^-. We found with a poor signal-to-noise ratio that the absorption spectrum of solvated electron in THF is also dramatically affected by the

Received: October 27, 2013
Revised: December 2, 2013
Published: December 2, 2013

presence of these complexed metal cations.[22] We used a simple asymptotic model assuming that solvated electron pairing with the ionic solutes yields absorption spectra with only one absorption band, but pairing with dipolar neutral solutes shows absorption spectra with two bands.

In the present study, we report new experimental results obtained by picosecond pulse radiolysis measurement. The fast decay of solvated electron is directly observed in pure THF solution and solutions containing Mg^{II}, Ca^{II}, and Sr^{II} salts. The absorption spectrum of solvated electron and further products are measured in a large domain from 400 to 1500 nm by using two configurations of the broadband pump probe setup, one in the visible and another one in the NIR range, with two types of line scan detectors. We show that the absorption spectra of the product between solvated electron and earth-alkaline cation depend on the type of the metal cation. Moreover, theoretical calculations are also performed to discuss if the monovalent earth alkaline metal cation is present or not as a transient in such conditions and if it is possible to reduce Mg^{II} by the solvated electron in ground or excited state. The simulated absorption spectra of the products are compared with experimental data and the details of electronic transitions are explained.

EXPERIMENTAL SECTION

Chemical. The purity of $Mg(ClO_4)_2$, $Ca(ClO_4)_2$ and $Sr(ClO_4)_2$ was greater than 99.9% and used as purchased from Sigma-Aldrich. THF solvent purity was 99.8% and purchased from ACS reagent and it was used as received.

Picosecond Pulse Radiolysis Setup. The experimental study was performed using the ELYSE laser-induced electron accelerator. The pulses are of 3−5 nC, 5−10 ps with an electron energy of 6−8 MeV at a repetition frequency of 10 Hz.[23,24] The transient absorbance was measured with a broadband pump−probe detection device, whose principle was already described elsewhere.[25] A short-lived absorbance due to the fused silica cell windows was detected in the empty cell when irradiated[26] and was subtracted from the absorbance data of the cell containing the THF samples.

The broadband pump−probe system was operated in two configurations, one for the visible using a single crystal of CaF_2 for continuum light generation and one using a single crystal of yttrium aluminum garnet (YAG) for continuum light generation optimized on the NIR. Probe and reference beam were each coupled into an optical fiber, transmitted to an adapted spectrometer, and dispersed onto the specific line scan detectors. For the measurements in the NIR, a customized broadband polychromator with an InGaAs photodiode array from Hamamatsu (G11608-512DA) was used.[27] Thanks to the new development and particularly the enhanced response down to the visible, spectral overlap of both detection configurations was achieved in the region below the fundamental laser wavelength of 780 nm.

The optical path of the flow cell is 0.5 cm. The time resolution is 15 ps (pulse width of electron pulse is around 7 ps). The dose per pulse is deduced from the absorbance of the hydrated electron e^-_{aq} in water, measured just before a series of experiments in THF. The dose was then derived from the yield at 15 ps,[28] $G(e^-_{aq})_{15\ ps} = 4.2 \times 10^{-7}$ mol J^{-1} and from the molar absorption coefficient $\varepsilon_{\lambda=800\ nm} = 1.53 \times 10^4$ L mol^{-1} cm^{-1}. The dose per pulse in water was around $D = 25$ Gy per pulse.

Data Analysis Method. The data matrices resulted from the averaging of about 50 scans, after removal of singular points resulting from outlier laser shots. They were then corrected for a wavelength-dependent baseline in order to be analyzed by a multivariate curve resolution alternating least-squares (MCR-ALS) approach.[29,30]

Because of the strong overlap between the spectra of the absorbing species in the present wavelength range, analysis of individual data matrices of experiments with cations was not able to unmix the specific components. In consequence, we implemented a data augmentation strategy, as follows.

Global matrices were built for each cation, by delay-wise binding the matrix for pure THF with the available matrices for this cation. In this configuration, the component spectra to be inferred are expected to be common to all the experiments in the global data set, while each experiment has its own set of kinetic traces. The presence of the pure THF matrix enables to single-out this component in the full set.

The number of absorbers in a global matrix was assessed by Singular Value Decomposition[31] of the global matrix, and a MCR-ALS analysis with the corresponding number of species (typically 2) was performed. Positivity constraints were imposed for both spectra and kinetics, and the kinetics of the cation in pure THF was constrained to be null. The residual maps were systematically inspected to assess the absence of model defects. The corresponding MCR-ALS code was adapted from the ALS package by Mullen.[32]

Theoretical Simulations of the Absorption Spectra. The presented measurements have prompted new calculations, based on state of the art molecular simulations. We have used a combination of the classical Monte Carlo code Gibbs[33] and of the quantum code Gaussian 09.[34] The $Mg(ClO_4)_2^-$ anion is placed in a polarized continuum medium (PCM) cavity in an implicit solvent. The implicit solvent is modeled with the solvent model using density (SMD) method[35] and is given the dielectric constant of THF (7.42). The Monte Carlo code generates a list of configurations according to the Metropolis algorithm at 300 K. We have used a large simulation box of 1000 Å. At each Mont Carlo step, a density functional theory (DFT) calculation is performed. We have used the B3LYP[36] functional and the SDD basis set,[37] supplemented with additional polarization and diffuse functions. For the MC simulations, we have added on each Cl and O atom one d (exponent 0.65) and one s and one p gaussians (exponent 0.08) and on the Mg atom one d (exponent 0.2) and one s and one p gaussians (exponent 0.0146). For the TDDFT (Time Dependent Density Functional Theory) calculations, we have added diffuse functions on the Mg atom: two s and p gaussians (exponents 0.007 and 0.003) and on Cl and O atoms one s and p gaussians, (exponent and 0.04).

The quantum calculation of the solute needs one minute for one MC step on our eight core machines. We could thus perform simulations with 20 000 MC steps and TDDFT calculations (with 20 excited states) every 50 MC step. In consequence, the final spectrum is the superposition of the 400 spectra of individual configurations. These spectra are superimposed with the help of a convolution with a Gaussian of full width at half-maximum (fwhm) 0.1 eV.

RESULTS

First, we present the absorption band observed in pure THF with picosecond pulse radiolysis measurements. The dose per pulse is obtained by measuring the absorbance of hydrated electron in the same conditions, by using the yield of hydrated electron at 15 ps (4.2×10^{-7} mol L^{-1} J^{-1}), and by taking into

dx.doi.org/10.1021/jp410598y | J. Phys. Chem. A 2013, 117, 14048−14055

account the electronic density of THF, which is less than that of water (0.884). The absorption band in pure THF is measured from 400 to 1500 nm using the two different probe configurations for the NIR and UV−visible (Figure 1). Under

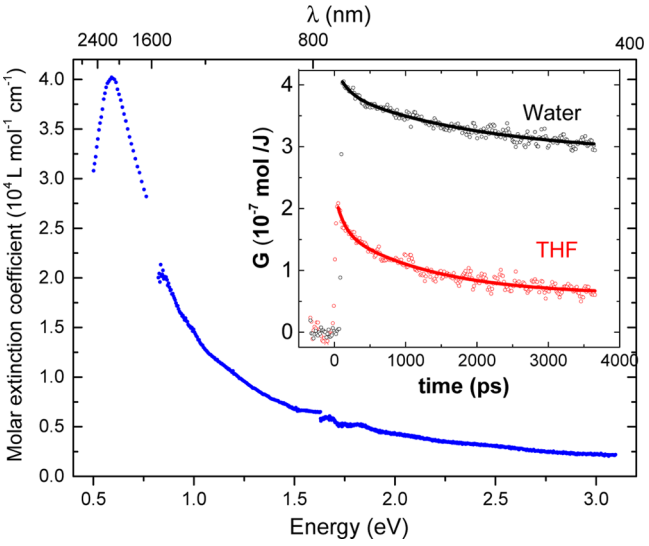

Figure 1. Absorption spectra of solvated electron in THF measured at 20 ps and scaled in molar extinction coefficient unit. The data from 1600 to 2400 nm are from Jou et al. obtained on the microsecond range[38] and those from 1600 to 400 nm are deduced from present work, which is in agreement with previous results obtained on the microsecond range. Inset: time dependent radiolytic yield of solvated electron in water and in THF.[38,40]

our experimental conditions, the concentration of the solvated electron at the end of the pulse is quite high (around 4×10^{-6} mol dm^{-3}). To be able to compete with reaction 1, the concentration of a solvated electron scavenger should be chosen high enough. Therefore, we observed the kinetics in solutions containing different concentrations of $M(ClO_4)_2$. Figure 2a−c reports the kinetics observed after the electron pulse at 730, 1000, and 1500 nm in THF solutions containing different concentration of magnesium perchlorate. Figure 3 reports the decays at the same wavelengths in THF solutions containing 0.05 M Mg^{II}, Ca^{II}, and Sr^{II}, respectively.

Figure 4 reports the absorption spectra obtained at 3.5 ns in solution containing 0.05 M cations. The overall absorption band of the three cases is large and it is constituted by several absorption bands.

DISCUSSION

All data obtained with pure THF and the three solutions containing 0.01, 0.05, and 0.1 M Mg^{II} are analyzed by SVD and show clearly that only two species are present in solution after the electron pulse, the solvated electron in pure THF and the product of the reaction with the solvated electron. In Figure 5, the absorption spectra of the two species obtained by MCR-ALS analysis and the kinetics for each solution and each species are reported. Similar results are obtained with two others salts in THF solutions.

In pure THF, the data analysis of the time-dependent absorption spectra shows that only one species absorbs in the range of 400 to 1500 nm. It is known that the solvated electron absorbs in the NIR. According to Dorfman et al. the maximum of the absorption band is located at 2160 nm with an extinction

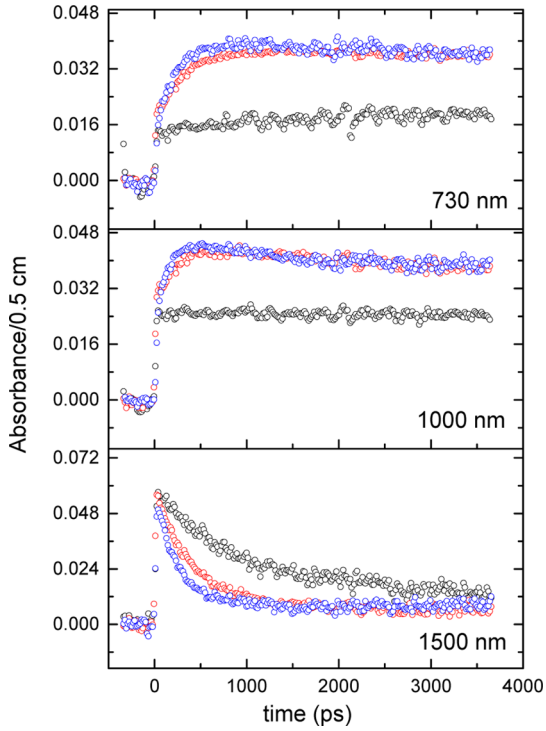

Figure 2. Picosecond pulse radiolysis absorbance measurements at 730, 1000, and 1500 nm in THF with 0.01 M $Mg(ClO_4)_2$ (black), 0.05 M $Mg(ClO_4)_2$ (red), and 0.1 M $Mg(ClO_4)_2$ (blue).

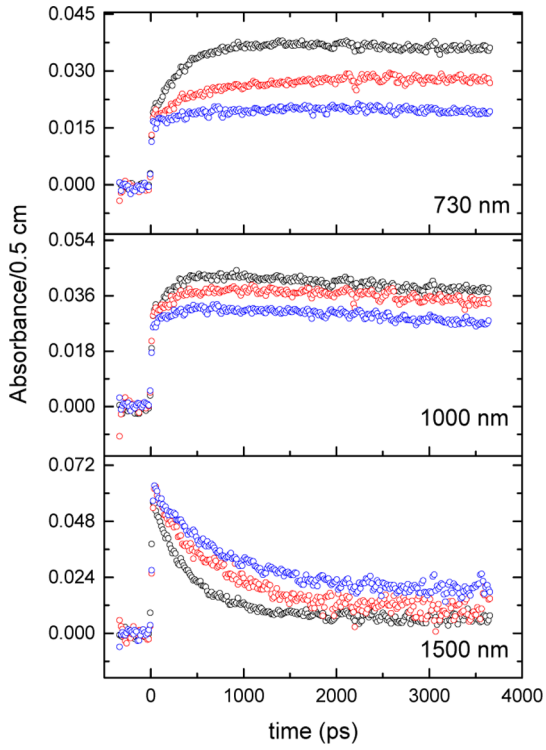

Figure 3. Picosecond pulse radiolysis absorbance measurements in THF solutions containing 0.05 M $Mg(ClO_4)_2$ (black), 0.05 M $Ca(ClO_4)_2$ (red), and 0.05 M $Sr(ClO_4)_2$ (blue).

coefficient of 40 000 M^{-1} cm^{-1}.[38] Our data from 400 to 1500 nm obtained at the picosecond range are in good agreement with the results already obtained from 550 to 2500 nm with microsecond pulse radiolysis (Figure 1).[38,39] Our data are also

dx.doi.org/10.1021/jp410598y | J. Phys. Chem. A 2013, 117, 14048−14055

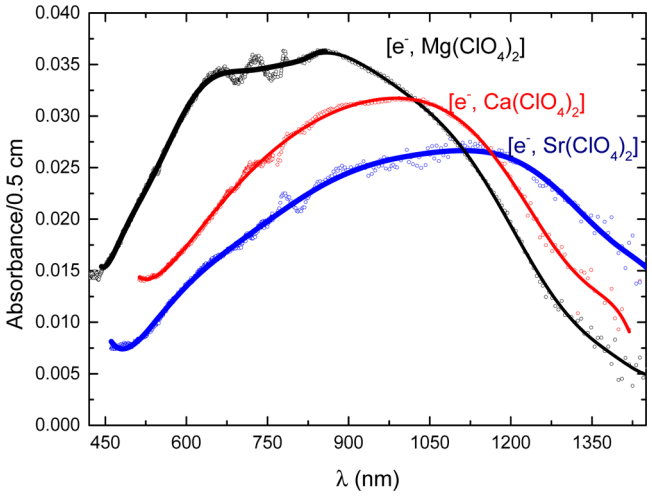

Figure 4. Absorption spectra recorded at 3.5 ns after the electron pulse in THF solution containing 0.05 M Mg^{II}, Ca^{II}, and Sr^{II}. The oscillations around 780 nm are due to the instability of the laser probe around the fundamental wavelength along the whole translation stage.

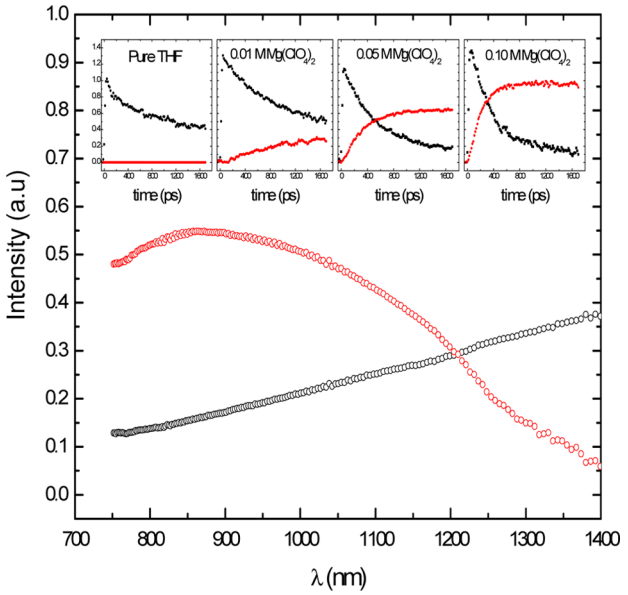

Figure 5. Absorption spectra and kinetics of the two transient species from the global MCR-ALS analysis of all data collected by picosecond pulse radiolysis measurement in pure THF, and solution containing Mg^{II} at 0.01, 0.05, and 0.1 mol L^{-1}.

in agreement with those reported by Saeki et al. from 500 to 800 nm by using a CCD camera in picosecond pulse radiolysis measurements.[40] Therefore, we consider that at short time in pure THF and also in solutions containing various concentration of $M^{II}(ClO_4)_2$ only solvated electron absorbs. It was shown that the absorption spectra of solvated electron can be fitted by a two Gaussian bands and a continuum tail. In our case also, the best fit is obtained with a generalized Lorentzian for higher energy side and a Gaussian for lower energy side of the absorption spectra (Figure 1). As reported by Schwartz et al. due to the molecular structure of THF, beside the ground state and first excited states in quasi-spherical cavity a multitude of others excited states exist with little Franck−Condon overlap with the ground state. That is why a simple Gaussian or Lorentzian function cannot reproduce the shape of the absorption band.

The radiolytic yield of solvated electron in pure THF is deduced from the decay and the value of the extinction coefficient of solvated electron (Figure 1, inset). At 15 ps, the yield of hydrated electron is around 4.2×10^{-7} mol L^{-1} J^{-1} but in THF it is only 2×10^{-7} mol L^{-1} J^{-1} and at 3.5 ns it decreases to 0.75×10^{-7} mol L^{-1} J^{-1}. The uncertainty on these values is mainly due to the value of the extinction coefficient of solvated electron in THF. The decay in THF is very fast compared with that of hydrated electron and it is mainly due to the reaction with THF^+ because of low dielectric constant and lower viscosity of THF than in water. Because of the time resolution of our setup, there is no access to the decay occurring during the first 15 ps. The value of the rate constant of this recombination reaction

$$e_s^- + THF^+ \rightarrow \text{Products} \quad (1)$$

is diffusion-controlled and larger than 10^{12} s^{-1} dm^{-3} mol^{-1}.[41] The nature of the hole, represented here by THF^+, is not known and it stands for all radical cations produced by the pulse. If we consider that the initial yield of ionization in solvent by low LET radiation is around 4.5×10^{-7} mol L^{-1} J^{-1} we have to consider that the presolvated electron in THF can react very quickly with the cation parent due to low solvent polarity and high diffusion of excess electron in THF. Therefore, more than 50% of electrons (presolvated and solvated) produced in THF recombine in less than 15 ps. Very efficient scavenging of precursor of solvated electron by biphenyl was previously reported.[40]

In solutions containing metal $M^{II}(ClO_4)_2$, the absorption spectra observed at 20 ps are identical to that obtained in pure THF and are due to that of solvated electron in THF. In the presence of Mg^{II}, the decay observed at 1500 nm becomes faster with increasing Mg^{II} concentration. The rate constant of the reaction between solvated electron and Mg^{II} deduced from the decay is 1.7×10^{10} mol^{-1} L s^{-1}. By increasing the concentration of Mg^{II} in THF solution, we observe that the kinetics at 730 and 1000 nm are also changing. At 730 nm, in pure THF only decay is observed but this decay is slowed down for 0.01 M solution and at higher concentration of Mg^{II}, even an increase of the absorbance is observed just after the electron pulse. The decay at 1000 nm is also slowed down drastically by increasing the Mg^{II} concentration and at highest concentration we observe an increase of the absorbance. The optical absorption spectra measured at 3.5 ns, show clearly the formation of the new species. The shape of the absorption band recorded at 3 ns depends on the solutions. For solutions containing Mg^{II}, a large absorption band with a shoulder at 1150 nm, and two bands at around 900 and 650 nm are observed.

The reaction occurring between the solvated electron and the cations Ca^{II} and Sr^{II} is slower than what we found with Mg^{II}. Compared to the absorption band of solvated electron, the shift to the visible is more important for the solution containing Mg^{II} and the lowest shift is observed for the solution containing Sr^{II}. The intensity of the absorbance is also more important for solutions containing Mg^{II}. This suggests that the equilibrium between the solvated electron and the pair depends on the earth alkaline metal cation. In the case of Mg^{II}, due to its lower size the pairs are more stable than in the two others cases.

It is known that in THF the salt cannot dissociate, and even for an initial concentration of 10^{-2} mol dm^{-3} of salt the

dx.doi.org/10.1021/jp410598y | J. Phys. Chem. A 2013, 117, 14048−14055

concentration of ionic species is very low. This indicates clearly that the reactions between the solvated electron and perchlorates in THF occur with the neutral form of the metallic salts, which is in huge excess compared to the ionic forms.

In the past, we performed Hartree–Fock calculations of the $Mg(ClO_4)_2$ in the presence of an excess electron in a spherical PCM cavity and found out that the electron did not reduce the solute, but rather stayed in the vicinity of it, forming a so-called contact electron-solute pair (noted $(Mg(ClO_4)_2, e^-)$).[22] We also found out that the perchlorate dissociation

$$(Mg(ClO_4)_2, e^-) \rightarrow MgO^+(ClO_3^-)(ClO_4^-) \quad (2)$$

is very favorable with $\Delta G = -2.7$ eV.[42]

We first tried to determine the structure of the absorbing species. To this aim we tried to optimize the geometry of the anionic solute $[Mg(ClO_4)_2]^-$ and found that the procedure always leads to the dissociated form MgO^+ of eq 2, whatever the (affordable) method used: B3LYP with large diffuse bases or MP2 with the aug-cc-pvtz basis. We have also supplemented the solute with up to eight explicit THF molecules, and again the geometry optimization led to the dissociated species.

We have therefore performed MC simulations with frozen geometries of the perchlorates. We have considered two geometries of these perchlorates, taken in the neutral $Mg(ClO_4)_2$ molecule with two bidentate ligands (its ground configuration) and two monodentate ligands (obtained with the help of a C_{3v} symmetry constraint. These two perchlorates differ from the isolated perchlorate by one or two elongated ClO bonds, designed to the MgO bonds; the monodentate perchlorate displays three short (1.49 Å) and one elongated bond (1.57 Å) and the bidentate perchlorate displays two short (1.49 Å) and two elongated bonds (1.57 Å).

The energy fluctuations for three simulations, initiated with two bidentate (hereafter noted bi–bi), one bi and one mono (bi– mono), and finally two monodentate perchlorates (mono–mono) are shown in Figure 6. It is worth noting that the simulations with the frozen perchlorates preserve their mono versus bidentate binding. This can be seen in Figure 7 where the MgCl g(r) have been displayed. For the bidentate perchlorate $g(r)$ ranges from 2.5 to 3 Å, for the monodentate perchlorate it ranges from 3 to 3.5 Å. It can be seen also that

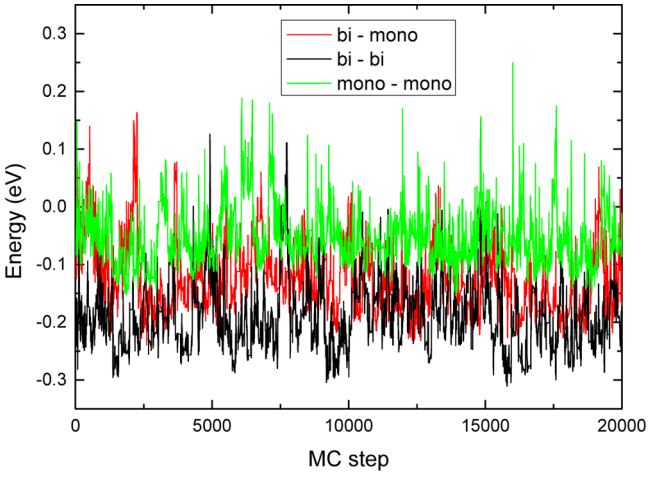

Figure 6. Energy fluctuations of the simulations with mono and bidentate perchlorates (the energy zero is set at −4320 eV).

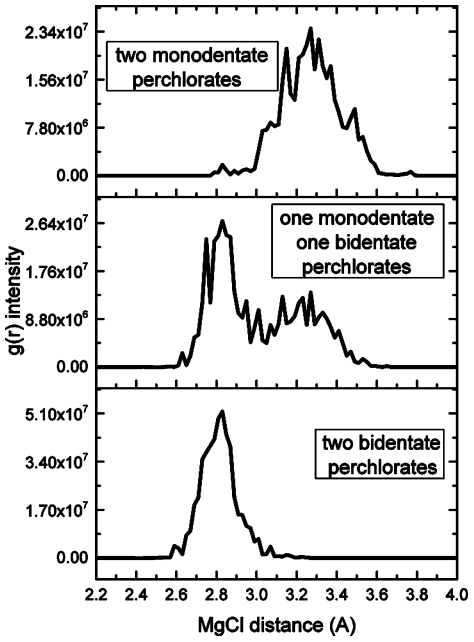

Figure 7. Mg–Cl $g(r)$ functions for the simulations with mono and bidentate perchlorates.

the bi–bi simulation is the most stable one, the mono–mono the less stable one, and that the bi–mono simulation lies above the bi–bi simulation, but close to it. The difference of the average energies of the bi–bi and bi–mono simulations amounts to 0.05 eV.

The absorption spectra corresponding to these three simulations are given in Figure 8 (top). It can be seen that the three simulations lead to very different spectra and that the spectrum of the bi–bi simulation is very similar to the experimental one with only a depression between 600 and 700 nm. It is worth noting that this depression is filled up by the spectrum of the bi–mono simulation. Nevertheless, the combination of the bi–bi and bi–mono spectra weighed by their Boltzmann factors hardly improves the calculated spectrum (Figure 9, bottom). In this combination, we have multiplied the Boltzmann factor of the bi–mono spectrum by a factor 2, because both bi–mono and mono–bi spectra actually interfere.

In Table 1, we give the TDDFT results for the two configurations of the bi–bi simulation, displaying the smallest value (conf. 10 450 in the MC list, 1312 nm) and the largest value (conf. 5000 in the MC list, 688 nm) of the first transition energy. The singly occupied molecular orbital (SOMO) and the first three virtual orbitals of these two configurations are shown in Figure 9. It is worth noting that the two SOMOs are somewhat different:

- For the configuration with a large energy transition, the orbital is essentially located on the side of the magnesium atom. In this case, the solute is exactly what we called in the past a contact electron solute pair.[22] In this case, we consider that the solute is not reduced by the solvated electron.
- For the configuration with a small transition energy, the orbital is located both on the side of the magnesium atom and on the perchlorates. For the sake of simplicity, we call this species an anion, though the reduction of the solute is only partial.

The present simulations therefore confirm and complement our first insights on this system.[22,42] The evaluation of the

dx.doi.org/10.1021/jp410598y | J. Phys. Chem. A 2013, 117, 14048–14055

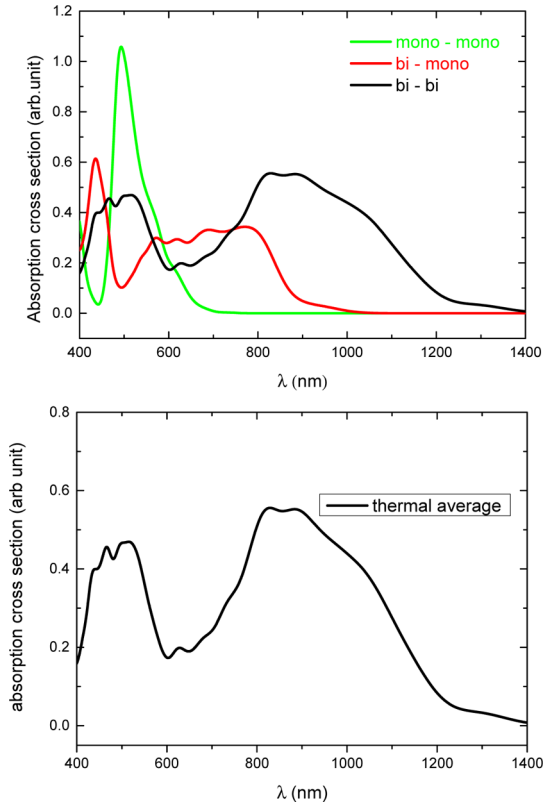

Figure 8. Absorption spectra for the species with mono and bidentate perchlorates.

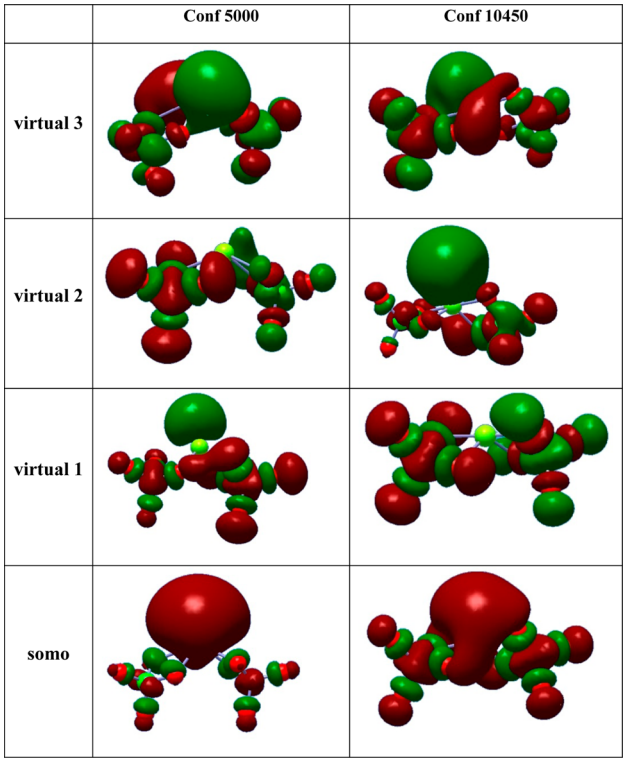

Figure 9. Isodensity surfaces of the SOMO and first three virtuals of the solute for two configurations with a large (conf. 5000, on the left) and with a small (conf. 10 450, on the right) value of the first transition energy.

Table 1. Transition Energies (eV), Wavelengths (nm), and Oscillator Strengths for Two Configurations with a large (conf. 5000) and with a Small Value (conf. 10 450) of the First Transition Energy

	conf. 5000			conf. 10450		
transition	ΔE	λ	f	ΔE	λ	f
1	1.802	688	0.1033	0.945	1312	0.1475
2	1.808	686	0.0879	1.148	1080	0.0403
3	1.984	625	0.0911	1.239	1000	0.0953

relative weights of these two species, contact pair and anion, is underway. Excitation of the electron from the SOMO toward the first two virtual orbitals (virtual orbitals and 1 and 2 of Figure 9) participates to the broad low energy band of the bi−bi spectrum. Excitation toward the third virtual (virtual orbital 3 of Figure 9) yields the band at 500 nm of the same spectrum. This third virtual is a rather clean p orbital of the Mg atom of A″ symmetry with respect of the ClMgCl plane of the solute; for this reason, the corresponding band is narrow and depends only slightly of the ligandation mode of the perchlorates, bi or monodentate.

CONCLUSION

Picosecond pulse radiolysis measurements of THF solutions containing different concentration of $Mg(ClO_4)_2$, $Ca(ClO_4)_2$, and $Sr(ClO_4)_2$ showed clearly that the reaction of solvated electron with these molecules yields into the formation of a new species absorbing in the NIR. Solvated electron is known to be the most reducing species in solvent, and our results show that it is possible to reduce the earth alkaline metal cation. In the case of magnesium, the interpretation of the measured absorption spectrum is made difficult by the fact that we have found no stable species for which a simulation can be performed, apart from the dissociated MgO^+ system.

We have performed MC simulations with constrained perchlorates and obtained an absorption spectrum remarkably close to the experimental one, apart from a depression at 650 nm. This success suggests the following conclusions and remarks:

- The absorbing species can be written $[Mg(ClO_4)_2]^-$. The fact that it can be observed suggests that it is trapped behind a potential barrier of a few tenths of electronvolts. We could not reproduce this barrier with ordinary quantum chemistry (DFT, MP2).
- This absorbing species undergoes oscillations between a contact pair and an anion. The contact pair displays high energy transitions and the anion displays low energy transitions. This results in a broad band between 600 and 1400 nm. In the pair, the solute is not reduced by the electron; in the anion it is partly reduced only.
- The depression at 650 nm in the calculated spectrum can be due to our freezing of the perchlorate geometries. It can also happen that B3LYP overestimates the transition energy of the band at 500 nm, or also that B3LYP underestimates the weight of the bi−mono spectrum in the final spectrum.

Mg^I is assumed to be one of the intermediaries during the formation of the Grignard compound formed by mixing metal powder magnesium and halide alky in THF solutions. Moreover Mg^I could play an important role in enzymatic mechanism. Therefore, these results could bring also new insight on the mechanism of Grignard compound formation and also Mg^{II} based enzyme.

dx.doi.org/10.1021/jp410598y | J. Phys. Chem. A 2013, 117, 14048−14055

■ ASSOCIATED CONTENT

Supporting Information

The detail of references 23 and 34 is given. This material is available free of charge via the Internet at http://pubs.acs.org.

■ AUTHOR INFORMATION

Corresponding Author

*E-mail: mehran.mostafavi@u-psud.fr,.

Notes

The authors declare no competing financial interest.

■ REFERENCES

(1) Hart, E. J.; Boag, J. W. Absorption Spectrum of the Hydrated Electron in Water and in Aqueous Solutions. *J. Am. Chem. Soc.* **1962**, *84*, 4090−4095.

(2) *Solvated Electron*; Gould, R. F., Ed.; Advances in Chemistry Series, No. 50; American Chemical Society: Washington, DC, 1965.

(3) Baxendale, J. H.; Wardaman, P. Direct Observation of Solvation of the Electron in Liquid Alcohols by Pulse Radiolysis. *Nature.* **1971**, *230*, 449−450.

(4) Chase, W. J.; Hunt, J .W. Solvation Time of The Electron in Polar Liquids. Water and Alcohols. *J. Phys. Chem.* **1975**, *79*, 2835−2845.

(5) Delaire, J. A.; Delcourt, M. O.; Belloni, J. Mobilities of Solvated Electrons in Polar Solvents from Scavenging Rate Constants. *J. Phys. Chem.* **1980**, *84*, 1186−1189.

(6) Holroyd, R. A. The Electron: its Properties and Reactions. In *Radiation Chemistry, Principles and Applications*; Farhaziz, Rodgers, M. A. J., Eds.; VCH: New York, 1987; p 201.

(7) Rossy, P. J.; Schnitker, J. The Hydrated Electron: Quantum Simulation of Structure, Spectroscopy, and Dynamic. *J. Phys. Chem.* **1988**, *92*, 4277−4285.

(8) Jou, F. Y.; Freeman, G. R. Shape of Optical Spectra of Solvated Electrons. Effect of Pressure. *J. Phys. Chem.* **1977**, *81*, 909−915.

(9) Schnitker, J.; Rossky, P. J. Quantum Simulation Study of the Hydrated Electron. *J. Chem. Phys.* **1987**, *86*, 3471−3485.

(10) Rossky, P. J.; Schnitker, J. The Hydrated Electron - Quantum Simulation of Structure, Spectroscopy, and Dynamics. *J. Phys. Chem.* **1988**, *92*, 4277−4285.

(11) Motakabbir, K. A.; Schnitker, J.; Rossky, P. J. Transient Photophysical Hole-Burning Spectroscopy of the Hydrated Electron - a Quantum Dynamical Simulation. *J. Chem. Phys.* **1989**, *90*, 6916−6924.

(12) Bratos, S.; Leicknam, J. C. Ultrafast Transient Absorption Spectroscopy of the Hydrated Electron: a Theory. *Chem. Phys. Lett.* **1996**, *261*, 117−122.

(13) Bratos, S.; Leicknam, J. C.; Borgis, D.; Staib, A. Subpicosecond Pump-Probe Absorption of the Hydrated Electron: Nonlinear Response Theory and Computer Simulation. *Phys. Rev. E.* **1997**, *55*, 7217−7227.

(14) Nicolas, C.; Boutin, A.; Levy, B.; Borgis, D. Molecular Simulation of a Hydrated Electron at Different Thermodynamic State Points. *J. Chem. Phys.* **2003**, *118*, 9689−9696.

(15) Buxton, G. V.; Greenstock, C. L.; Helman, W. P.; Ross, A. B. Critical-Review of Rate Constants for Reactions of Hydrated Electrons, Hydrogen-Atoms and Hydroxyl Radicals (•OH/•O^-) in Aqueous-Solution. *J. Phys. Chem. Ref. Data.* **1988**, *17*, 513−886.

(16) Buxton, G. V.; Mulazzani, Q. G.; Ross, A. B. Critical-Review of Rate Constants for Reactions of Transients from Metal-Ions and Metal-Complexes in Aqueous-Solution. *J. Phys. Chem. Ref. Data.* **1995**, *24*, 1055−1349.

(17) Bram, G.; Peralez, E.; Negrel, J. C.; Chanon, M. Victor Grignard and the Birth of his Reagent. *C.R. Acad. Sci. Paris* **1997**, *325*, 235−240.

(18) Bickelhaupt, F. Organomagnesium Chemistry - Nearly 100 Years but Still Fascinating. *J. Organomet. Chem.* **1994**, *475*, 1−14.

(19) Garst, J.; Hungvary, F. In *Grignard Reagents. New Developments*; Richey, H. G., Ed.; J. Wiley: New York, 2000.

(20) Kruczynski, T.; Pushkarevsky, N.; Henke, P.; Koppe, R.; Baum, E.; Konchenko, S.; Pikies, J.; Schnockel, H. Hunting for the Magnesium(I) Species: Formation, Structure, and Reactivity of some Donor-Free Grignard Compounds. *Angew. Chem., Int. Ed.* **2012**, *51*, 9025−9029.

(21) Renou, F.; Mostafavi, M. Reactivity of the Solvated Electron toward Divalent Magnesium. *Chem. Phys. Lett* . **2001**, *335*, 363−368.

(22) Renou, F.; Mostafavi, M.; Archirel, P.; Bonazzola, L.; Pernot, P. Solvated Electron Pairing with Earth Alkaline Metals in THF. 1. Formation and Structure of the Pair with Divalent Magnesium. *J. Phys. Chem. A.* **2003**, *107*, 1506−1516.

(23) Belloni, J.; Monard, H.; Gobert, F.; Larbre, J. P.; Demarque, A.; De Waele, V.; Lampre, I.; Marignier, J. L.; Mostafavi, M.; Bourdon, J. C.; et al. ELYSE - A Picosecond Electron Accelerator for Pulse Radiolysis Research. *Nucl. Instrum. Methods Phys. Res., Sect. A* **2005**, *539*, 527−539.

(24) Marignier, J. L.; de Waele, V.; Monard, H.; Gobert, F.; Larbre, J. P.; Demarque, A.; Mostafavi, M.; Belloni, J. Time-Resolved Spectroscopy at the Picosecond Laser-Triggered Electron Accelerator ELYSE. *Radiat. Phys. Chem.* **2006**, *75*, 1024−1033.

(25) Schmidhammer, U.; Pernot, P.; De Waele, V.; Jeunesse, P.; Demarque, A.; Murata, S.; Mostafavi, M. Distance Dependence of the Reaction Rate for the Reduction of Metal Cations by Solvated Electrons: a Picosecond Pulse Radiolysis Study. *J. Phys. Chem. A* **2010**, *114*, 12042−12051.

(26) Schmidhammer, U.; El Omar, A. K.; Balcerzyk, A.; Mostafavi, M. Transient Absorption Induced by a Picosecond Electron Pulse in the Fused Silica Windows of an Optical Cell. *Radiat. Phys. Chem.* **2012**, *81*, 1715−1719.

(27) Schmidhammer, U.; Jeunesse, P.; Stresing, G.; Mostafavi, M. A Broadband Ultrafast Transient Absorption Spectrometer Covering the Near-Infrared (NIR) Down to the Green. *Appl. Spectrosc.* Submitted for publication, **2013**.

(28) Muroya, Y.; Lin, M. Z.; Wu, G. Z.; Iijima, H.; Yoshi, K.; Ueda, T.; Kudo, H.; Katsumura, Y. A Re-evaluation of the Initial Yield of the Hydrated Electron in the Picosecond Time Range. *Radiat. Phys. Chem.* **2005**, *72*, 169−172.

(29) Tauler, R. Multivariate Curve Resolution Applied to Second Order Data. *Chemom. Intell. Lab. Syst.* **1995**, *30*, 133−146.

(30) Ruckebusch, C.; Sliwa, M.; Pernot, P.; de Juan, A.; Tauler, R. Comprehensive Data Analysis of Femtosecond Transient Absorption Spectra: A Review. *J. Photochem. Photobiol. C* **2012**, *13*, 1−27.

(31) Golub, G. H.; Van Loan, C. F. *Matrix Computation*, 2nd ed.; The John Hopkins University Press: London, 1989.

(32) Mullen, K.M. ALS: Multivariate Curve Resolution Alternating Least Squares (MCR-ALS). R package version 0.0.5. http://CRAN.R-project.org/package=ALS] in the R language [R Core Team (2012). R: A language and environment for statistical computing; R Foundation for Statistical Computing, Vienna, Austria, 2012; http://www.R-project.org.

(33) Ungerer, P.; Tavitian, B.; Boutin, A. Applications of Molecular Simulation in the Oil and Gas Industry Monte Carlo Methods, Editions Technip: Paris, 2005.

(34) Frisch, M. J.; Trucks, G. W.; Schlegel, H. B.; Scuseria, G. E.; Robb, M. A.; Cheeseman, J. R.; Scalmani, G.; Barone, V.; Mennucci, B.; Petersson, G. A.; Nakatsuji, H.; Caricato, M.; Li, X.; Hratchian, H. P.; Izmaylov, A. F.; Bloino, J.; Zheng, G.; Sonnenberg, J. L.; Hada, M.; Ehara, M.; Toyota, K.; Fukuda, R.; Hasegawa, J.; Ishida, M.; Nakajima, T.; Honda, Y.; Kitao, O.; Nakai, H.; Vreven, T.; Montgomery, J. A., Jr.; Peralta, P. E.; Ogliaro, F.; Bearpark, M.; Heyd, J. J.; Brothers, E.; Kudin, K. N.; Staroverov, V. N.; Kobayashi, R.; Normand, J.; Raghavachari, K.; Rendell, A.; Burant, J. C.; Iyengar, S. S.; Tomasi, J.; Cossi, M.; Rega, N.; Millam, N. J.; Klene, M.; Knox, J. E.; Cross, J. B.; Bakken, V.; Adamo, C.; Jaramillo, J.; Gomperts, R.; Stratmann, R. E.; Yazyev, O.; Austin, A. J.; Cammi, R.; Pomelli, C.; Ochterski, J. W.; Martin, R. L.; Morokuma, K.; Zakrzewski, V. G.; Voth, G. A.; Salvador, P.; Dannenberg, J. J.; Dapprich, S.; Daniels, A. D.; Farkas, Ö.; Ortiz, J. V.; Cioslowski, J.; Fox, D. J. *Gaussian 09*, revision A.02 ; Gaussian, Inc.: Wallingford, CT, 2009.

(35) Marenich, A. V.; Cramer, C. J.; Truhlar, D. J. Universal Solvation Model Based on Solute Electron Density and on a Continuum Model of the Solvent Defined by the Bulk Dielectric Constant and Atomic Surface Tensions. *J. Phys. Chem. B* **2009**, *113*, 6378−6396.
(36) Becke, A. D. Density-Functional Thermochemistry 0.3. the Role of Exact Exchange. *J. Chem. Phys.* **1993**, *98*, 5648−5652.
(37) Fuentealba, P.; Preuss, H.; Stoll, H.; Szentpaly, L. A Proper Account of Core-polarization with Pseudopotentials: Single Valence-Electron Alkali Compounds. *Chem. Phys. Lett.* **1989**, *89*, 418−422.
(38) Jou, F. Y.; Dorfman, L. M. Pulse radiolysis studies. XXI. Optical Absorption Spectrum of the Solvated Electron in Ethers and in Binary Solutions of these Ethers. *J. Chem. Phys.* **1973**, *58*, 4715−4723.
(39) Salmon, G. A.; Sedddon, W. A.; Fletcher, J. W. Pulse Radiolysis of Solvated Electrons, Ions Pairs, and Alkali Metal Anions in Tetrahydrofuran. *Can. J. Chem.* **1974**, *52*, 3259−3268.
(40) Saeki, A.; Kozawa, T.; Ohnishi, Y.; Tagawa, S. Reactivity between Biphenyl and Precursor of Solvated Electron in THF Measured by Picosecond Pulse Radiolysis in Near-Ultraviolet Visible and Infrared. *J. Phys. Chem. A* **2007**, *111*, 1229−1235.
(41) Cipollini, N. E.; Holroyd, R. A.; Nishikawa, M. Zero Field Mobility of Excess Electrons in Dense Methane Gas. *J. Chem. Phys.* **1977**, *67*, 4636−4639.
(42) Renou, F.; Archirel, P.; Pernot, P.; Lévy, B.; Mostafavi, M. Pulse Radiolysis Study of Solvated Electron Pairing with Alkaline Earth Metals in Tetrahydrofuran. 3. Splitting of p-like Excited States of Solvated Electron Perturbed by Metal Cations. *J. Phys. Chem. A* **2004**, *108*, 987−995.